

## SPECTRAL BEHAVIOR OF COMBUSTION FRONTS WITH HIGH EXOTHERMICITY\*

ANNA GHAZARYAN<sup>†</sup>, JEFFREY HUMPHREYS<sup>‡</sup>, AND JOSHUA LYTLE<sup>‡</sup>

**Abstract.** We study fronts in a reaction-diffusion model for high Lewis number combustion processes with the reaction rate in the form of an Arrhenius law. By a combination of spectral energy estimates and Evans function computation, we study the unstable spectrum of a class of combustion fronts with high exothermicity, where the previously known results do not apply and interesting spectral behavior is observed.

**Key words.** high Lewis number, combustion fronts, Evans function, spectral stability

**AMS subject classifications.** 80A25, 35K57, 35B35, 35C07, 35P15

**DOI.** 10.1137/120864891

**1. Introduction.** We consider a reaction-diffusion system introduced in [49] as a model for the propagation of combustion waves in one spatial dimension  $x \in \mathbb{R}$ , in the case of a premixed gaseous fuel with the assumption of no heat loss. The system describing the time ( $t \geq 0$ ) evolution of the scaled temperature  $u = u(x, t)$  and concentration of the fuel  $y = y(x, t)$  is given by

$$(1) \quad \begin{aligned} u_t &= u_{xx} + y\Omega(u), \\ y_t &= \varepsilon y_{xx} - \beta y\Omega(u), \end{aligned}$$

where  $\varepsilon = 1/\text{Le} \geq 0$  is the reciprocal of the Lewis number and represents the ratio of the fuel diffusivity to the heat diffusivity,  $\beta > 0$  is the exothermicity, which is the ratio of the activation energy to the heat of the reaction, and  $\Omega(u)$  is the ignition function

$$\Omega(u) = \begin{cases} e^{-1/u} & \text{for } u > 0, \\ 0 & \text{otherwise,} \end{cases}$$

which is a smooth Arrhenius law, where the reaction starts at the ambient temperature  $u = 0$ .

Historically (see, for example, [12] or [50]), systems describing combustion of premixed fuels involve the temperature variable scaled to be 1 at the physical maximum. System (1) originated as a result of a nontraditional nondimensionalization procedure which led to physical values of temperature varying between 0 and  $\frac{1}{\beta}$ . Investigation of (1) in a series of papers [49, 5, 46, 19, 21, 43] significantly complemented the information obtained for the traditional system (see [41, 7, 33, 38]).

We consider system (1) posed on one-dimensional physical space. Not only does it describe the burning of a premixed fuel arranged in a one-dimensional configuration, for example, in an insulated long cylinder, but it also serves as a reasonable

\*Received by the editors February 6, 2012; accepted for publication (in revised form) December 10, 2012; published electronically February 14, 2013.

<http://www.siam.org/journals/siap/73-1/86489.html>

<sup>†</sup>Department of Mathematics, Miami University, Oxford, OH 45056 (ghazarar@muohio.edu). This author was supported in part by National Science Foundation, grant DMS-0908009.

<sup>‡</sup>Department of Mathematics, Brigham Young University, Provo, UT 84602 (jeffh@math.byu.edu, joshualyte@gmail.com). These authors were supported in part by National Science Foundation, grant DMS-CAREER-0847074.

approximation for steady planar combustion waves undergoing longitudinal perturbations. Indeed, in [35] and [36] it has been shown that when  $Le > 1$  ( $\varepsilon < 1$ ) the transverse instabilities do not develop. The planar fronts themselves are of interest in pyrotechnic systems [10].

The system (1) with  $\varepsilon = 0$  ( $Le = \infty$ ) is usually used to describe combustion of solid fuels or, more precisely, combustion that involves the solid phase only with no gaseous products present. In the case of  $0 < \varepsilon \ll 1$ , that is, when  $Le$  is large but finite, (1) describes the burning of high density fluids at high temperatures. Finally, gaseous combustion is characterized by larger values of  $\varepsilon \approx 1$ . In this paper, we consider combustion fronts with  $0 < \varepsilon \ll 1$  fixed.

The system (1) is related to a system where the reaction rate  $\Omega(u)$  is replaced by  $H(u - u_{ign})\Omega(u)$ , where  $H$  is the Heaviside function and  $u_{ign}$  is the ignition temperature. This modified system has been studied, for example, in [7]. The introduction of the ignition temperature changes properties of the system related to the existence of the fronts drastically. In the system with an ignition temperature the front is unique up to translation [7] while, as we will discuss below, the system with no ignition has a continuum of waves for all speeds faster than some critical speed. The earliest results [18, 28, 47, 38, 37] on traveling waves in (1) are about the case  $\varepsilon = 1$ , when the system can be reduced to a scalar equation. The multiplicity of solutions was later on shown for more general  $\varepsilon$ , but the system with ignition temperature helps to discriminate between the continuum of waves of (1). The slowest front of (1) appears to be a limit of fronts in the ignition type of systems as the ignition temperature goes to zero (see [38]). For  $\varepsilon$  sufficiently small, that slowest front also happens to be the only one that converges to both of its rest states exponentially. The latter is a technical convenience from the point of view of the methods (such as Evans function calculation) that we use. In this paper, neither the bounds on the eigenvalues, nor our numerical calculation of those is influenced by introduction of a cutoff at a sufficiently small ignition temperature.

Exothermicity determines how much fuel has to be burned to achieve a unit increase in the temperature. We discuss below the stability of combustion fronts with high exothermicity values. In fact, it is well known that for a certain critical value of  $\beta = \beta_\varepsilon^*$ , for fixed  $\varepsilon$ , there is a Hopf-like bifurcation where a conjugate pair of eigenvalues (of the linearized operator of the wave) crosses the imaginary axis into the right-hand side. Physically, for one-dimensional fronts and for planar fronts in two-dimensional space under one-dimensional perturbations along the front, these eigenvalues indicate a pulsating instability [41, 39]. In the case of two-dimensional perturbations, the instability is expected to manifest itself as transversally propagating wavetrains [3, 40]. The onset of this instability was studied in [5] using Evans function methods [1], which determine the unstable eigenvalues of the linearized operator about the combustion profile; see also [49, 43, 46]. The goal of this paper is to examine the spectral behavior of one-dimensional combustion fronts for values of high exothermicity. In particular, it was of interest to us to explore whether the oscillatory nature of the instability persists with the increase of the exothermicity parameter.

This paper is organized as follows. In section 2 we review the previous work on this model, and examine the existence and stability problems for combustion fronts. Of particular interest is the spectral stability of the front, which is determined by examining the spectrum of the differential operator obtained by linearizing the PDE about the traveling wave. The spectrum of this linearized operator is analyzed in section 3. We first determine the location of the essential spectrum and its effect on the stability. Then, by using spectral energy estimates, we show that the unstable

eigenvalue bounds converge to zero as  $\beta$  gets large. However, since the eigenvalues cross transversely into the right-hand side at  $\beta = \beta_\varepsilon^*$ , this suggests that they either turn back toward the origin or cross back to the left half-plane. In section 4 we verify our analytical work by tracking the unstable eigenvalues through Evans function computation. We show that these eigenvalues converge to the origin, after coalescing and then splitting again on the real axis. In the parameter regime where the eigenvalues are real the instability is not expected to be oscillatory.

## 2. Background.

**2.1. Traveling wave equations.** Combustion fronts of (1) can be identified by translating into a moving coordinate frame  $x \rightarrow x - ct$  and considering steady-state solutions of

$$(2) \quad \begin{aligned} u_t &= u_{xx} + cu_x + y\Omega(u), \\ y_t &= \varepsilon y_{xx} + cy_x - \beta y\Omega(u). \end{aligned}$$

More precisely, a combustion front is a solution to the ordinary differential system

$$(3) \quad \begin{aligned} u'' + cu' + y\Omega(u) &= 0, \\ \varepsilon y'' + cy' - \beta y\Omega(u) &= 0. \end{aligned}$$

We remark that the parameter  $c$  represents the wave speed of the front, which is initially unknown, but can, without loss of generality, be assumed positive.

Obviously, this system has infinitely many equilibria of the form  $(u, y)$  with  $u \leq 0$  and  $(u, 0)$  for any  $u \in \mathbb{R}$ . For the meaningful, from the physical point of view, equilibria  $u \geq 0$  and  $0 \leq y \leq 1$ , but of a special interest is the front that invades the equilibrium which represents the unburned state  $(u, y) = (0, 1)$  and leaves behind a state where all of the fuel is spent,  $(u, y) = (\bar{u}, 0)$ . The value of  $\bar{u}$  will be described below. Therefore, at  $+\infty$  we impose on the front the boundary condition  $(u, y)(+\infty) = (0, 1)$ .

The system (3) has a conserved quantity  $\beta u' + \beta c u + \varepsilon y' + c y$ , which defines a family of invariant sets  $\beta u' + \beta c u + \varepsilon y' + c y = \text{constant}$ . Among these, only

$$(4) \quad \beta u' + \beta c u + \varepsilon y' + c y = c$$

contains the equilibrium point  $(0, 1)$ . On the other hand, the only equilibrium of the form  $(\bar{u}, 0)$  that belongs to the invariant set (4) is defined by  $\bar{u} = 1/\beta$ .

To summarize, we study solutions of (3) subject to the boundary conditions

$$(5) \quad (u, y)(-\infty) = (1/\beta, 0) \quad \text{and} \quad (u, y)(+\infty) = (0, 1).$$

This represents a heteroclinic orbit asymptotically connecting the completely burned state, where  $y = 0$  and the temperature  $u = \frac{1}{\beta}$  is maximal, and the unburned state at the ambient temperature  $u = 0$ . We remark that the conserved quantity (4) will be used below in numerically computing the solution to (3)–(5).

In the remainder of this section, we discuss past literature on the existence and stability properties of the combustion fronts, and set up our spectral analysis to follow.

**2.2. The existence of combustion fronts.** The existence problem for (3)–(5) has been well studied. Speaking generally, the existence and uniqueness (up to translation) literature for this model can be broken into three groups, namely, the

infinite Lewis number case ( $\varepsilon = 0$ ), the high Lewis number case ( $0 < \varepsilon \ll 1$ ), and the more general case  $\varepsilon > 0$ , where other asymptotic limits are commonly employed.

In an appropriate scaling, (3) falls into the class of equations described in [7], where Leray–Schauder degree theory was been used to prove the existence of the front for  $0 < \varepsilon < 1$ . When  $\beta = 1$  and  $\varepsilon = 0$  the existence of the fronts has been shown in [33] using methods similar to those of [7]. Other studies of involving both  $\varepsilon = 0$  and  $\varepsilon > 0$  have been carried out in special cases by using phase-plane and asymptotic analysis; see, for example, [21, 29, 8, 38, 37, 48, 34, 2]. Numerical studies for  $\varepsilon = 0$  and  $\varepsilon > 0$  have also been carried out; see, for example, [49, 5]. It has been shown that fronts exist for a continuum of speeds, but only one (up to translation) of them converges to its rest states exponentially fast. The rest of the profiles converge to the rest states algebraically and are viewed as of little physical interest; see [48, 21] for details. This is in agreement with the analysis carried out for the case of  $\epsilon = 1$  in [38], where it has been shown that an introduction of an arbitrary small ignition cutoff in the function describing the reaction rate leads to a unique up to translation wave [27, 18, 47] which converges as the ignition cutoff approaches 0 to the slowest front, which coincides with the front with exponential decay at  $\pm\infty$ . Throughout this paper, we consider only solutions which decay exponentially to their end states.

For  $0 < \varepsilon \ll 1$ , an essentially different approach to the proof of the existence and uniqueness of the front can be based on geometric singular perturbation theory [28], since (3) has a slow-fast structure. In the limiting case of  $\varepsilon = 0$ , the flow is restricted to a two-dimensional invariant manifold, which is normally hyperbolic and attracting. Therefore, by Fenichel's first theorem [17], it perturbs to an attracting manifold invariant for the flow with  $\varepsilon > 0$ . For the reduced problem, the lower dimension of the problem can be used to show that the front in the  $\varepsilon = 0$  case is formed as a transversal intersection of relevant invariant manifolds [21]. Transversality can be proved by Melnikov integral calculation [5], or directly as in [20].

Several papers have also examined the dependence of the wave speed on the exothermicity; see, for example, [5, 43, 49, 48]. Several similar approximate formulas have been obtained, each describing exponential convergence  $c \rightarrow 0$  as  $\beta \rightarrow \infty$ . We also know that combustion fronts  $(\hat{u}, \hat{y})$ , when they exist for  $c > 0$ , satisfy  $\hat{u}(x) > 0$  and  $\hat{y}(x) > 0$  for  $x \in \mathbb{R}$  and both  $\hat{u}$  and  $\hat{y}$  are monotone in  $x$ ; see [38, 46] for  $\varepsilon > 0$  and [34] for  $\varepsilon = 0$ .

**2.3. The stability of the combustion front.** The slow-fast structure of the wave has been used, not only to prove the existence and uniqueness of the front for the perturbed system, but also to show that the spectrum of the front with sufficiently small  $\varepsilon > 0$  is a perturbation of order  $\varepsilon$  of the spectrum of the front with  $\varepsilon = 0$  [19].

The front possesses essential spectrum up to the imaginary axis; therefore, even in a parameter regime that guarantees absence of the unstable discrete spectrum, spectral information is not definitive. There exists an exponentially weighted norm that stabilizes the front on the linear level. The nonlinear stability in that exponentially weighted norm was proven in [22]. The result describes the instability caused by unstable essential spectrum as convective. In contrast to spectral information, linear and nonlinear stability analyses of the front for  $\varepsilon = 0$  and  $0 < \varepsilon \ll 1$  call for essentially different approaches due to significantly different properties of the linearized operators. The case of  $\varepsilon > 0$  is discussed below, whereas the  $\varepsilon = 0$  case is discussed in [21].

The linearization of (2) about the combustion front  $(\hat{u}, \hat{y})$  is given by

$$(6a) \quad u_t = u_{xx} + cu_x + e^{-1/\hat{u}}y + \hat{y}\hat{u}^{-2}e^{-1/\hat{u}}u,$$

$$(6b) \quad y_t = \varepsilon y_{xx} + cy_x - \beta e^{-1/\hat{u}}y - \beta \hat{y}\hat{u}^{-2}e^{-1/\hat{u}}u.$$

The eigenvalue problem reads

$$(7a) \quad \lambda u = u_{xx} + cu_x + e^{-1/\hat{u}}y + \hat{y}\hat{u}^{-2}e^{-1/\hat{u}}u,$$

$$(7b) \quad \lambda y = \varepsilon y_{xx} + cy_x - \beta e^{-1/\hat{u}}y - \beta\hat{y}\hat{u}^{-2}e^{-1/\hat{u}}u.$$

A traveling wave is called spectrally stable if the spectrum of the linearization of the system about the traveling wave is contained in the left half-plane  $\{\lambda \in \mathbb{C} \mid \operatorname{Re} \lambda < 0\} \cup \{0\}$ . Generally speaking, the spectral stability need not imply the linear stability of the traveling wave, i.e., the decay of the solutions of the linearized PDE (6).

If the linearized operator is sectorial, linear stability is guaranteed if there exists  $\eta > 0$  such that the spectrum belongs to the half-plane  $\{\lambda \in \mathbb{C} \mid \operatorname{Re} \lambda < -\eta\}$  with the exception of a simple eigenvalue at zero that is due to translation symmetry. For (7) with sufficiently small  $\varepsilon > 0$  it has been shown in [19] using the *stability index* [1] that the translational eigenvalue  $\lambda = 0$  is simple. The proof is based on the reduction of the stability analysis of the case  $0 < \varepsilon \ll 1$  to the stability analysis of the case  $\varepsilon = 0$ . For  $\varepsilon = 0$  the multiplicity of the zero eigenvalue is calculated in [21] using the Evans function. Numerical investigations [43, 5, 46], for both  $\varepsilon = 0$  and  $\varepsilon > 0$ , also confirm that the translational eigenvalue is simple.

There is numerical evidence that the discrete spectrum of the front strongly depends on the parameter  $\beta$  [43]. Specifically, for fixed  $\varepsilon > 0$ , there exists  $\beta_\varepsilon^*$  such that no unstable discrete spectrum exists when  $\beta < \beta_\varepsilon^*$ , and a pair of complex conjugate eigenvalues crosses the imaginary axis from left to right when  $\beta = \beta_\varepsilon^*$ . As  $\beta$  increases, the complex-conjugated eigenvalue pair moves into the right-hand side of the complex plane. In this paper, we show that as  $\beta$  further increases the eigenvalues turn back, collide on the real axis, and then converge toward the origin along the real axis in the limit as  $\beta \rightarrow \infty$ .

The parameter regime  $\beta < \beta_\varepsilon^*$  has been thoroughly studied. Although no unstable eigenvalues are present, the essential spectrum of the front extends all the way to the imaginary axis. For  $\varepsilon > 0$  it touches the imaginary axis at the origin and for  $\varepsilon = 0$  it include all of the imaginary axis, so the front is spectrally stable in certain exponentially weighted norms and only for the class of perturbations which decay at  $+\infty$  faster than at a certain exponential rate. For fixed  $\varepsilon > 0$  the linearized operator is a perturbation of the Laplacian by lower-order derivatives and bounded operators and, thus, it is sectorial [24, 45]. Therefore, the linear stability of the front in appropriate exponentially weighted spaces follows from the spectral stability. This is not the case for the system with  $\varepsilon = 0$  where the spectrum of the linearized operator contains a vertical line (the imaginary axis) and therefore the linearized operator is not sectorial; see [21] for details. The nonlinear stability does not simply follow from the linear stability because of the insufficient smoothness of the nonlinearity in the weighted space. Nevertheless, this issue is resolved in [22, 21], where it is shown that the front is nonlinearly stable in the weighted norm against perturbations that are sufficiently small both in the weighted  $H^1$  norm and the regular  $H^1$  norm without a weight and that belong to the subspace complementary to the span of the derivative of the front, i.e., central direction. Stability in an exponential norm implies convective character of the instability of the front.  $H^1$  norm or sup-norm of perturbations do not, in general, decay in time exponentially. More precisely, it is the temperature component of the perturbation that cannot be expected to decay in time exponentially, but only by diffusion, at an algebraic rate. Nevertheless, in the co-moving frame perturbations are transported to the equilibria at  $-\infty$ , so a pointwise decay of perturbations is observed. When  $\beta \geq \beta_\varepsilon^*$ , unstable discrete eigenvalues cause much stronger, absolute

instability when the perturbations grow exponentially fast in  $H^1$  norm and, in the co-moving frame, no pointwise decay takes place.

The occurrence of a Hopf-like bifurcation for  $\beta = \beta_\varepsilon^*$  has been discussed in [46]. We note that this is not a generic case of a Hopf bifurcation because, in addition to a pair of isolated eigenvalues crossing the imaginary axis, the essential spectrum is touching the imaginary axis for all  $\beta$ . In this paper we will be interested in what happens for values of  $\beta$  which are larger than any considered in the literature.

The numerical observation of this instability is not unexpected. Its presence has been proved under the assumption of high-energy activation [41]. In this situation, the existence of two complex-conjugate, purely imaginary eigenvalues has been obtained. But in some way, the behavior of the unstable eigenvalues as functions of  $\beta$ , when  $\beta$  is large, has not been completely captured by the numerics in [43]. In other words, it is not clear from the numerics what happens with the unstable eigenvalues for  $\beta \gg 1$ . Based on our estimates in section 3.2, we claim that with further increase of  $\beta$ , at some point, the radius of the unstable eigenvalues start to decrease. The eigenvalues become real and approach the origin along the real axis when  $\beta$  is increased.

**3. The spectrum of the linearized operator.** In this section, we show that (i) the essential spectrum belongs to the closed left half-plane, and (ii) that the unstable eigenvalue bounds converge to zero as  $\beta$  gets large, thus restricting the spectrum to only low-frequency instabilities.

**3.1. The essential spectrum.** The right-hand side of (7) can be expressed as the differential operator

$$(8) \quad \mathcal{L} = \begin{pmatrix} \partial_{xx} + c\partial_x + \hat{y}\hat{u}^{-2}e^{-1/\hat{u}} & e^{-1/\hat{u}} \\ -\beta\hat{y}\hat{u}^{-2}e^{-1/\hat{u}} & \varepsilon\partial_{xx} + c\partial_x - \beta e^{-1/\hat{u}} \end{pmatrix}.$$

The spectrum of this operator consists of the essential spectrum and the point spectrum. The essential spectrum is connected with far-field behavior and is defined by the dynamics at the rest states of the front; therefore, alongside with (8), we consider the limiting operators

$$(9) \quad \mathcal{L}_\pm = \lim_{x \rightarrow \pm\infty} \mathcal{L} = \begin{pmatrix} \partial_{xx} + c\partial_x & (e^{-1/\hat{u}})_\pm \\ 0 & \varepsilon\partial_{xx} + c\partial_x - \beta(e^{-1/\hat{u}})_\pm \end{pmatrix}.$$

To determine the rightmost points in the essential spectrum of  $\mathcal{L}(\xi)$ , it suffices to compute the essential spectra of  $\mathcal{L}^\pm$ . These spectra can be calculated using the Fourier transform

$$(10) \quad \widehat{\mathcal{L}}_\pm = \begin{pmatrix} -\xi^2 + ic\xi & (e^{-1/\hat{u}})_\pm \\ 0 & -\varepsilon\xi^2 + ic\xi - \beta(e^{-1/\hat{u}})_\pm \end{pmatrix}.$$

A complex number  $\lambda$  is in the spectrum of  $\widehat{\mathcal{L}}_\pm$  if and only if there is a nonzero vector  $v$  and a number  $\xi \in \mathbb{R}$  so that  $\lambda v = \widehat{\mathcal{L}}_\pm v$  or, equivalently,

$$(11) \quad \det \begin{pmatrix} -\xi^2 + ic\xi - \lambda & (e^{-1/\hat{u}})_\pm \\ 0 & -\varepsilon\xi^2 + ic\xi - \beta(e^{-1/\hat{u}})_\pm - \lambda \end{pmatrix} = 0.$$

Thus, the rightmost curve is the parabola

$$(12) \quad \lambda(\xi) = -\min\{\varepsilon, 1\}\xi^2 + ic\xi$$

which bounds the essential spectrum [24]. The region to the right of this parabola then contains only discrete spectra, that is, isolated eigenvalues of finite multiplicity [46].

We remark that the parabola (12) touches the imaginary axis, and thus spectral stability can only be achieved in some exponentially weighted subspace of  $L^2$  and not  $L^2$  itself (see the discussion in section 2.3), but our goal is to study strongly unstable cases characterized by the presence of exponentially growing modes due to eigenvalues with positive real parts.

**3.2. Spectral energy estimates.** In the remainder of this section, we show that there are spectral bounds that converge to zero in the infinite  $\beta$  limit. The temporal eigenvalues are  $\lambda \in \mathbb{C}$  such that system (7) has a nontrivial, localized at  $\pm\infty$ , solution  $(\hat{u}, \hat{y})$ .

LEMMA 1. *If  $(u, y)$  satisfies (7) for some nonzero  $\lambda$  with  $\operatorname{Re}(\lambda) \geq 0$ , then the following two inequalities hold for all  $\varepsilon_1 > 0$ :*

$$(13) \quad \operatorname{Re}(\lambda) \int |u|^2 \leq \int \frac{\hat{y}}{\hat{u}^2} e^{-1/\hat{u}} |u|^2 + \varepsilon_1 \int e^{-1/\hat{u}} |u|^2 + \frac{1}{4\varepsilon_1} \int e^{-1/\hat{u}} |y|^2$$

and

$$(14) \quad (\operatorname{Re}(\lambda) + |\operatorname{Im}(\lambda)|) \int |u|^2 \leq \frac{c^2}{4} \int |u|^2 + \int \left( \frac{\hat{y}}{\hat{u}^2} + \varepsilon_1 \right) e^{-1/\hat{u}} |u|^2 + \frac{1}{2\varepsilon_1} \int e^{-1/\hat{u}} |y|^2.$$

*Proof.* We multiply (7a) by the conjugate  $\bar{u}$  and integrate from  $-\infty$  to  $\infty$ . Thus we have

$$(15) \quad \lambda \int |u|^2 = c \int u' \bar{u} + \int \frac{\hat{y}}{\hat{u}^2} e^{-1/\hat{u}} |u|^2 + \int e^{-1/\hat{u}} y \bar{u} - \int |u'|^2.$$

Taking the real and imaginary parts of (15), respectively, and simplifying, we have

$$(16a) \quad \operatorname{Re}(\lambda) \int |u|^2 = \int \frac{\hat{y}}{\hat{u}^2} e^{-1/\hat{u}} |u|^2 + \operatorname{Re} \int e^{-1/\hat{u}} y \bar{u} - \int |u'|^2,$$

$$(16b) \quad |\operatorname{Im}(\lambda)| \int |u|^2 \leq c \int |u'| |u| + \left| \operatorname{Im} \int e^{-1/\hat{u}} y \bar{u} \right|.$$

The inequality (13) follows by using Young's inequality on (16a). The inequality (14) follows by adding (16a) and (16b) together and using Young's inequality to get

$$\begin{aligned} (\operatorname{Re}(\lambda) + |\operatorname{Im}(\lambda)|) \int |u|^2 &\leq \frac{c^2}{4} \int |u|^2 + \int \frac{\hat{y}}{\hat{u}^2} e^{-1/\hat{u}} |u|^2 + \sqrt{2} \int e^{-1/\hat{u}} |u| |y| \\ &\leq \frac{c^2}{4} \int |u|^2 + \int \left( \frac{\hat{y}}{\hat{u}^2} + \varepsilon_1 \right) e^{-1/\hat{u}} |u|^2 \\ &\quad + \frac{1}{2\varepsilon_1} \int e^{-1/\hat{u}} |y|^2. \quad \square \end{aligned}$$

LEMMA 2. *If  $(u, y)$  satisfies (7) for some nonzero  $\lambda$  with  $\operatorname{Re}(\lambda) \geq 0$ , then the following inequalities hold for all  $\varepsilon_2 > 0$ :*

$$(17) \quad \operatorname{Re}(\lambda) \int |y|^2 + \beta \int e^{-1/\hat{u}} |y|^2 \leq \varepsilon_2 \beta \int \frac{\hat{y}}{\hat{u}^2} e^{-1/\hat{u}} |u|^2 + \frac{\beta}{4\varepsilon_2} \int \frac{\hat{y}}{\hat{u}^2} e^{-1/\hat{u}} |y|^2$$

and

$$(18) \quad (\operatorname{Re}(\lambda) + |\operatorname{Im}(\lambda)|) \int |y|^2 \leq \frac{c^2}{4\varepsilon} \int |y|^2 + \varepsilon_2 \beta \int \frac{\hat{y}}{\hat{u}^2} e^{-1/\hat{u}} |u|^2 + \beta \int \left( \frac{\hat{y}}{2\varepsilon_2 \hat{u}^2} - 1 \right) e^{-1/\hat{u}} |y|^2.$$

*Proof.* We multiply (7b) by the conjugate  $\bar{y}$  and integrate from  $-\infty$  to  $\infty$ . Thus we have

$$(19) \quad \lambda \int |y|^2 = c \int y' \bar{y} - \beta \int \frac{\hat{y}}{\hat{u}^2} e^{-1/\hat{u}} u \bar{y} - \beta \int e^{-1/\hat{u}} |y|^2 - \varepsilon \int |y'|^2.$$

Taking the real and imaginary parts of (19), respectively, and simplifying, we have

$$(20a) \quad \operatorname{Re}(\lambda) \int |y|^2 = -\beta \operatorname{Re} \int \frac{\hat{y}}{\hat{u}^2} e^{-1/\hat{u}} u \bar{y} - \beta \int e^{-1/\hat{u}} |y|^2 - \varepsilon \int |y'|^2,$$

$$(20b) \quad |\operatorname{Im}(\lambda)| \int |y|^2 \leq c \int |y'| |y| + \beta \left| \operatorname{Im} \int \frac{\hat{y}}{\hat{u}^2} e^{-1/\hat{u}} u \bar{y} \right|.$$

The inequality (17) follows by using Young's inequality on (20a). The inequality (18) follows by adding (20a) and (20b) together and using Young's inequality to get

$$\begin{aligned} & (\operatorname{Re}(\lambda) + |\operatorname{Im}(\lambda)|) \int |y|^2 \\ & \leq \frac{c^2}{4\varepsilon} \int |y|^2 + \sqrt{2}\beta \int \frac{\hat{y}}{\hat{u}^2} e^{-1/\hat{u}} |u| |y| - \beta \int e^{-1/\hat{u}} |y|^2 \\ & \leq \frac{c^2}{4\varepsilon} \int |y|^2 + \varepsilon_2 \beta \int \frac{\hat{y}}{\hat{u}^2} e^{-1/\hat{u}} |u|^2 + \beta \int \left( \frac{\hat{y}}{2\varepsilon_2 \hat{u}^2} - 1 \right) e^{-1/\hat{u}} |y|^2. \quad \square \end{aligned}$$

**THEOREM 3.** *If  $(u, y)$  satisfies (7) for some nonzero  $\lambda$  with  $\operatorname{Re}(\lambda) \geq 0$ , then the following inequalities hold for all  $0 < \delta < 1$  and for  $\beta \geq 2$ :*

$$(21) \quad \operatorname{Re}(\lambda) < \left( \frac{\beta^2}{1-\delta} + \frac{(1-\delta)^2 \beta}{16\delta} \right) e^{-\beta}$$

and

$$(22) \quad \operatorname{Re}(\lambda) + |\operatorname{Im}(\lambda)| < \frac{c^2}{4} \max \left\{ 1, \frac{1}{\varepsilon} \right\} + \left( \frac{\beta^2}{1-\delta} + \frac{(1-\delta)^2 \beta}{4\delta} \right) e^{-\beta}.$$

Together these inequalities form a trapezoidal region of admissible unstable spectrum, whose area vanishes for large  $\beta$ .

*Proof.* To prove (21), we multiply (13) by  $\theta$  and add to (17). Hence,

$$\begin{aligned} \operatorname{Re}(\lambda) \int (\theta |u|^2 + |y|^2) & \leq (\theta + \beta \varepsilon_2) \int \frac{\hat{y}}{\hat{u}^2} e^{-1/\hat{u}} |u|^2 + \varepsilon_1 \int e^{-1/\hat{u}} \theta |u|^2 \\ & + \left( \frac{\theta}{4\varepsilon_1} - \beta \right) \int e^{-1/\hat{u}} |y|^2 + \frac{\beta}{4\varepsilon_2} \int \frac{\hat{y}}{\hat{u}^2} e^{-1/\hat{u}} |y|^2. \end{aligned}$$

Setting  $\varepsilon_1 = \frac{\theta}{4\beta}$ ,  $\varepsilon_2 = \frac{(1-\delta)\beta}{4}$ , and  $\theta = \frac{(1-\delta)^2 \beta^2}{4\delta}$ , we have that

$$\operatorname{Re}(\lambda) \int (\theta |u|^2 + |y|^2) \leq \frac{1}{1-\delta} \int \frac{\hat{y}}{\hat{u}^2} e^{-1/\hat{u}} (\theta |u|^2 + |y|^2) + \frac{(1-\delta)^2 \beta}{16\delta} \int e^{-1/\hat{u}} \theta |u|^2.$$

Note that  $e^{-1/\hat{u}} < e^{-\beta}$  and  $\hat{u}^{-2}e^{-1/\hat{u}} \leq \beta^2 e^{-\beta}$ ,  $\beta \geq 2$ . Thus,

$$(23) \quad \operatorname{Re}(\lambda) \leq \frac{1}{1-\delta} \sup_x \frac{\hat{y}}{\hat{u}^2} e^{-1/\hat{u}} + \frac{(1-\delta)^2 \beta}{16\delta} \sup_x e^{-1/\hat{u}} \leq \left( \frac{\beta^2}{1-\delta} + \frac{(1-\delta)^2 \beta}{16\delta} \right) e^{-\beta}.$$

To prove (22), we multiply (14) by  $\theta$  and add to (18). Hence,

$$\begin{aligned} & (\operatorname{Re}(\lambda) + |\operatorname{Im}(\lambda)|) \int (\theta|u|^2 + |y|^2) \\ & \leq \frac{c^2}{4} \max \left\{ 1, \frac{1}{\varepsilon} \right\} \int (\theta|u|^2 + |y|^2) \\ & \quad + \left( \frac{\theta}{2\varepsilon_1} - \beta \right) \int e^{-1/\hat{u}} |y|^2 + \left( 1 + \frac{\beta\varepsilon_2}{\theta} \right) \int \frac{\hat{y}}{\hat{u}^2} e^{-1/\hat{u}} \theta|u|^2 \\ & \quad + \varepsilon_1 \int e^{-1/\hat{u}} \theta|u|^2 + \frac{\beta}{2\varepsilon_2} \int \frac{\hat{y}}{\hat{u}^2} e^{-1/\hat{u}} |y|^2. \end{aligned}$$

This time we set  $\varepsilon_1 = \frac{\theta}{2\beta}$ ,  $\varepsilon_2 = \frac{(1-\delta)\beta}{2}$ , and  $\theta = \frac{(1-\delta)^2\beta^2}{2\delta}$ , and obtain

$$\begin{aligned} & (\operatorname{Re}(\lambda) + |\operatorname{Im}(\lambda)|) \int (\theta|u|^2 + |y|^2) \\ & \leq \frac{c^2}{4} \max \left\{ 1, \frac{1}{\varepsilon} \right\} \int (\theta|u|^2 + |y|^2) \\ & \quad + \frac{1}{1-\delta} \int \frac{\hat{y}}{\hat{u}^2} e^{-1/\hat{u}} (\theta|u|^2 + |y|^2) + \frac{(1-\delta)^2 \beta}{4\delta} \int e^{-1/\hat{u}} \theta|u|^2. \end{aligned}$$

This yields

$$\begin{aligned} & (\operatorname{Re}(\lambda) + |\operatorname{Im}(\lambda)|) < \frac{c^2}{4} \max \left\{ 1, \frac{1}{\varepsilon} \right\} + \frac{1}{1-\delta} \sup_x \frac{\hat{y}}{\hat{u}^2} e^{-1/\hat{u}} + \frac{(1-\delta)^2 \beta}{4\delta} \sup_x e^{-1/\hat{u}} \\ & \leq \frac{c^2}{4} \max \left\{ 1, \frac{1}{\varepsilon} \right\} + \left( \frac{\beta^2}{1-\delta} + \frac{(1-\delta)^2 \beta}{4\delta} \right) e^{-\beta}. \quad \square \end{aligned}$$

*Remark 4.* According to the numerical investigations in [5], when the parameter  $\beta$  is increased beyond  $\beta_\varepsilon^*$ , a pair of complex eigenvalues crosses the imaginary axis and moves into the unstable half-plane of the complex plane. Our estimate (21) shows that as  $\beta$  is increased even further, the eigenvalues must turn back and move toward the imaginary axis. With the added result that the wave speed  $c > 0$  converges to zero in the large  $\beta$  limit [5, 43, 49, 48], it follows from (22) that the bounds on the imaginary part also converge to zero. Thus, we have that these unstable eigenvalues either converge to the origin or pass back through the imaginary axis resulting in stable high-exothermicity combustion fronts. In the following section, we demonstrate numerically that the eigenvalues remain unstable and converge to the origin, and hence the combustion fronts remain unstable for all  $\beta > \beta_\varepsilon^*$ .

*Remark 5.* We also know from [48, section 3] that there are high-frequency bounds in the  $\varepsilon = 0$  case. This has been extended to  $\varepsilon \ll 1$  in [19], through a geometric singular perturbation argument. The results in (21) and (22) are sharper and hold for all values of  $\varepsilon > 0$  and  $\beta > 0$ .

**4. Numerical results.** In this section, we describe our numerical Evans function study for combustion fronts of (1). Recall that the Evans function  $D(\lambda)$  is

analytic to the right of the essential spectrum and is defined as the Wronskian of decaying solutions of the eigenvalue equation for the linearized system (7). Similar to the characteristic polynomial, the Evans function satisfies  $D(\lambda) = 0$  if and only if  $\lambda$  is an eigenvalue of (7); see [1] for a detailed mathematical description. Thus the study of the point spectrum of combustion fronts in (1) reduces to the problem of locating and tracking the roots of the Evans function  $D(\lambda)$  as parameters vary. Although the Evans function is generally too complex to compute exactly, it can be well-approximated numerically, even for large systems [26, 31, 32].

Since  $D(\lambda)$  is analytic in the right half-plane, we can detect the unstable eigenvalues of the system by counting and locating its roots using winding-number computations. As a result, we can observe the onset of instability of a front by tracking eigenvalues as they cross into the right-hand side of the complex plane. This approach was used first by Evans and Feroe [16] and has since been applied to other systems. In fact, Evans function computation is on its way to becoming a mature technology. All of the numerical investigations in this paper were performed using specially adapted portions of the numerical library STABLAB [6].

In this paper, we examine the eigenvalue behavior well beyond the onset of instability. Specifically, we track numerically the eigenvalues in the large exothermicity limit, where they cross into the right half-plane, and then turn around and converge to the origin, thus confirming the behavior suggested by the energy estimates in section 3.2.

**4.1. Computation of combustion fronts.** Before one can evaluate the Evans function, the front itself must be computed. We begin by letting  $z_1 = \hat{u}$ ,  $z_2 = \hat{u}'$ ,  $z_3 = \hat{y}$ , and  $z_4 = \hat{y}'$ , and expressing (3) as a first-order system

$$(24) \quad \begin{pmatrix} z_1 \\ z_2 \\ z_3 \\ z_4 \end{pmatrix}' = \begin{pmatrix} z_2 \\ -cz_2 - z_3 e^{-1/z_1} \\ z_4 \\ \frac{1}{\varepsilon}(-cz_4 + \beta z_3 e^{-1/z_1}) \end{pmatrix},$$

subject to the boundary conditions (5). Note that the constant of motion (4) reduces (24) to the system  $U' = f(U)$ , where

$$(25) \quad U = \begin{pmatrix} z_1 \\ z_2 \\ z_4 \end{pmatrix} \quad \text{and} \quad f(U) = \begin{pmatrix} z_2 \\ -cz_2 - \frac{1}{c}(c - \beta cz_1 - \beta z_2 - \varepsilon z_4)e^{-1/z_1} \\ \frac{1}{\varepsilon} \left[ -cz_4 + \frac{\beta}{c}(c - \beta cz_1 - \beta z_2 - \varepsilon z_4)e^{-1/z_1} \right] \end{pmatrix},$$

with boundary conditions

$$U_- := U(-\infty) = \begin{pmatrix} 1 \\ \beta \\ 0 \\ 0 \end{pmatrix} \quad \text{and} \quad U_+ := U(+\infty) = \begin{pmatrix} 0 \\ 0 \\ 0 \\ 0 \end{pmatrix}.$$

Since combustion fronts are heteroclinic orbits, there is a continuum of solutions given by translation in  $x$ . Thus, to single out a single (canonical) solution, we add the additional condition that  $z_1(0) = \hat{u}(0) = \beta^{-1}/2$  so that the combustion front is “centered” at the origin. Then we truncate the real line to a sufficiently large interval  $[-L, L]$  so that the desired solutions have sufficiently decayed to the end states. Since

the desired profile converges exponentially to its end states, the requisite values of  $L$  are usually modest in size.

To ensure that the numerical solution connects the unstable manifold at  $x = -\infty$  to the stable manifold at  $x = +\infty$ , we use projective boundary conditions at  $\pm L$  given by  $\Pi_{\pm}(U(\pm L) - U_{\pm}) = 0$ , where  $\Pi_{\pm}$  is a matrix of orthonormal vectors spanning the complementary eigenspaces of  $dF(U_{\pm})$ . More precisely, we project out the two-dimensional stable manifold at  $x = -\infty$  and the one-dimensional center manifold at  $x = \infty$ . With the conditions at  $x = \pm L$ , together with the centering condition at  $x = 0$ , this is a three-point boundary-value problem. A clever trick to simplify the problem is to double the size of the three-dimensional system and halve the domain, thus going from

$$U' = f(U), \quad x \in [-L, L], \quad U \in \mathbb{R}^3,$$

to the six-dimensional system

$$\begin{pmatrix} U \\ V \end{pmatrix}' = \begin{pmatrix} f(U) \\ -f(V) \end{pmatrix}, \quad x \in [-L, 0], \quad U, V \in \mathbb{R}^3,$$

together with the three “matching” conditions  $U(0) = V(0)$ . Since the centering and matching conditions both occur at  $x = 0$ , we have reduced the problem to a two-point boundary-value problem, for which several numerical packages exist; see, for example, [4, 14].

*Remark 6.* Two common techniques for computing two-point boundary-value problems are shooting and collocation methods. In this paper, we use a (nonnative) MATLAB package `bvp6c`, which is a sixth-order collocation method for solving two-point boundary-value problems and can be called from STABLAB; see [23] for details. Throughout the paper, we set the absolute and relative tolerances to be  $10^{-9}$  and  $10^{-8}$ , respectively.

Another wrinkle in the problem is that the wave speed  $c$  is unknown. Thus, we add another ODE to the system,  $c' = 0$ . Hence, to find the profile, we use a two-point boundary-value solver on the seven-dimensional system

$$\begin{pmatrix} U \\ V \\ c \end{pmatrix}' = \begin{pmatrix} f(U) \\ -f(V) \\ 0 \end{pmatrix}, \quad x \in [-L, 0], \quad U, V \in \mathbb{R}^n,$$

subject to the seven boundary conditions: two projective conditions at  $x = -L$ , a single projective condition at  $x = L$ , the three matching conditions  $U(0) = V(0)$ , and the above centering condition. This gives an equal number of variables and boundary conditions. Thus, all that is needed to solve the combustion profile is a sufficiently close guess that will converge. This is a significant challenge for many of the desired parameters of this problem.

Using numerical continuation, however, we can use the solution in one parameter regime to find the solution in a more difficult regime. In other words, once a solution is found for a certain parameter, one can slightly change the parameter and use the previous solution (or a variation of the previous solution) as the guess for the new parameter and get the new solution. In Figure 1, we see a typical profile. Here we have that  $\beta = 7.2$ ,  $\varepsilon = 0.1$ , and  $c = 0.0228$ .

**4.2. Evans function computation.** We briefly describe how to compute the Evans function. We begin by writing the eigenvalue problem (7) as a first-order linear

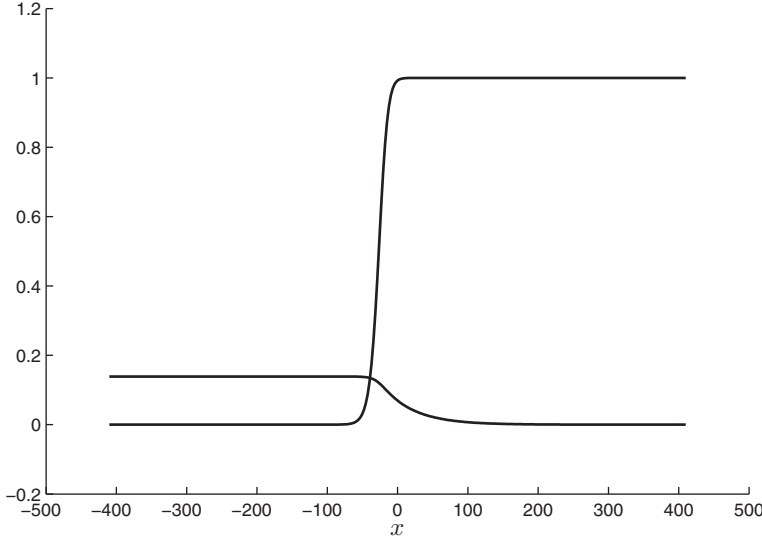


FIG. 1. Combustion front for  $\beta = 7.2$ ,  $\varepsilon = 0.1$ , and  $c = 0.0228$ .

system

$$(26) \quad W' = A(x, \lambda)W,$$

where

$$A(x, \lambda) = \begin{pmatrix} 0 & 1 & 0 & 0 \\ \lambda + \hat{y}\hat{u}^{-2}e^{-1/\hat{u}} & -c & -e^{-1/\hat{u}} & 0 \\ 0 & 0 & 0 & 1 \\ \frac{\beta}{\varepsilon}\hat{y}\hat{u}^{-2}e^{-1/\hat{u}} & 0 & \frac{1}{\varepsilon}(\lambda + \beta e^{-1/\hat{u}}) & -\frac{c}{\varepsilon} \end{pmatrix}, \quad W = \begin{pmatrix} u \\ u' \\ y \\ y' \end{pmatrix}, \quad ' = \frac{d}{dx}.$$

We note that an eigenvalue of (7) corresponds to a nontrivial solution  $W(x)$  of (26) satisfying the boundary conditions  $W(\pm\infty) = 0$ . For a given nonzero  $\lambda$  satisfying  $\text{Re}(\lambda) \geq 0$ , this occurs when the manifold evolving from the two-dimensional unstable subspace  $W_1^- \wedge W_2^-$  of (26) at  $x = -\infty$  intersects at  $x = 0$  with the manifold evolving (backward) from the two-dimensional stable subspace  $W_3^+ \wedge W_4^+$  of (26) at  $x = \infty$ . Intersection occurs if and only if the volume form  $W_1^- \wedge W_2^- \wedge W_3^+ \wedge W_4^+$  equals zero. Since the volume form is dual to the determinant, we can define the Evans function as  $D(\lambda) := \det(W_1^-, W_2^-, W_3^+, W_4^+)_{|x=0}$ . We remark that throughout the region of interest, the subspaces are analytically varying, and thus the Evans function is also analytic. Hence, the roots correspond, in terms of both location and multiplicity, to the eigenvalues of (7); see [1] for a complete mathematical description.

Numerically, there are two major challenges to computing the Evans function: first is to ensure that the initializing vectors  $\{W_1^-(\infty), W_2^-(\infty)\}$  and  $\{W_3^+(\infty), W_4^+(\infty)\}$  are analytic in  $\lambda$ . This is resolved using Kato's method, which uses the stable and unstable spectral projections of  $A(\pm\infty, \lambda)$ , which are analytic, to uniquely evolve the above basis vectors as  $\lambda$  varies; see [30, p. 99] for a mathematical description and [25, 51, 6] for details on the numerical implementation.

The second numerical challenge is overcoming the stiffness of the linear ODE (26). For an arbitrary choice of two initializing vectors  $W_1^-(\infty)$  and  $W_2^-(\infty)$  at

$x = -\infty$ , we find that naive numerical integration will result in the errors favoring the direction of the largest growth mode. Hence, the approximate trajectories over time will become asymptotically colinear and badly conditioned as a result. The classical approach to resolving this issue is to use the compound-matrix method, which lifts (26) to a six-dimensional wedge-product space, where single trajectories correspond to the evolution of the 2-forms above. This is the approach taken in [49, 43], and leads to good numerical computations.

In this paper, we use instead the analytic orthogonalization (or polar coordinate) method described in [26] and fashioned in part after the continuous orthogonalization method of Drury [15] and Davey [13]. This technique tracks the evolution of the requisite 2-form by solving the nonlinear ODE

$$(27) \quad \Omega'_{\pm}(x) = (I - \Omega_{\pm}(x)\Omega_{\pm}(x)^*)A(x, \lambda)\Omega_{\pm}(x),$$

where each  $\Omega_{\pm}$  is a  $4 \times 2$  evolutionary matrix that tracks the same subspace in orthogonal coordinates. This together with the scalar ODE

$$(28) \quad \gamma'_{\pm}(x) = \text{tr}(\Omega_{\pm}(x)^* A(x, \lambda)\Omega_{\pm}(x))\gamma_{\pm}(x)$$

provides the necessary analytic corrector, which satisfies for all  $x$  the following:

$$\begin{aligned} W_1^- \wedge W_2^- &= \gamma_-(\Omega_1^- \wedge \Omega_2^-), \\ W_3^+ \wedge W_4^+ &= \gamma_+(\Omega_3^+ \wedge \Omega_4^+). \end{aligned}$$

Thus, the Evans function takes the form of

$$(29) \quad D(\lambda) = \gamma_- \gamma_+ \det(\Omega_-, \Omega_+) |_{x=0},$$

where  $\Omega_- = (\Omega_1^- \Omega_2^-)$  and  $\Omega_+ = (\Omega_3^+ \Omega_4^+)$  are  $4 \times 2$  matrices. We initialize this method at  $x = \pm\infty$  by using any one of several orthogonal decomposition methods (such as the QR or polar decompositions) that yield  $W_- = (W_1^- W_2^-) = \Omega_- \alpha_-$  and  $W_+ = (W_3^+ W_4^+) = \Omega_+ \alpha_+$ , where  $\alpha_{\pm}$  are  $2 \times 2$  matrices and  $\gamma_{\pm} = \det \alpha_{\pm}$ .

*Remark 7.* Once the initial vectors at  $x = \pm L$  are computed, we use the MATLAB package `ode45`, which is called from STABLAB, to integrate (27)–(28) from  $\pm L$  to zero, and then (29) is evaluated. We remark that the absolute and relative tolerances for the integration were also set to be  $10^{-9}$  and  $10^{-8}$ , respectively.

**4.3. Rootfinding for  $D(\lambda)$ .** Root finding in Evans function computation can be performed using the method of moments as described in [44, 9, 42, 11]. As a generalization of the argument principle in complex analysis, we have the following: Let  $f$  be analytic inside and on a simple closed positively oriented curve  $\Gamma$ . If  $f$  is nonzero on  $\Gamma$  and  $z_1, \dots, z_n$  are the roots of  $f(z)$  inside  $\Gamma$ , then the  $p$ th moment of  $f$  about  $z^*$  is given by

$$(30) \quad M_p(z^*) = \frac{1}{2\pi i} \oint_{\Gamma} \frac{(z - z^*)^p f'(z)}{f(z)} = \sum_{k=1}^n (z_k - z^*)^p.$$

Specifically,  $M_0(0) = n$  gives the number of roots inside  $\Gamma$ ,  $M_1(0) = z_1 + z_2 + \dots + z_n$  gives the sum of the roots, and  $M_2(0) = z_1^2 + z_2^2 + \dots + z_n^2$  is the sum of the squares of the roots. Thus, we can determine the location of any unstable eigenvalues by computing (30) numerically, via Simpson's rule or any higher-order quadrature method, for various contours.

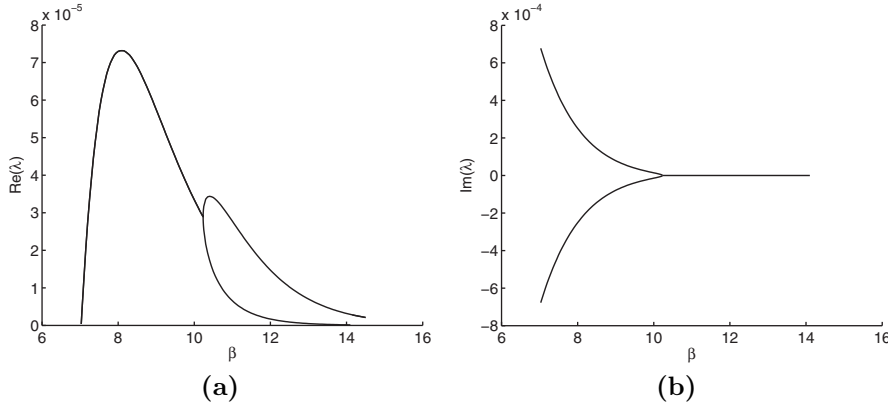


FIG. 2. The graphs of unstable roots as determined by Evans function computation for combustion fronts with  $\varepsilon = 0.1$  and  $\beta$  varying in the interval [7.026, 14.1]. Both the (a) real and (b) imaginary parts of  $\lambda$  are graphed as a function of  $\beta$ . Note that a conjugate pair of eigenvalues crosses the imaginary axis transversely at approximately  $\lambda = \pm 6.8i \times 10^{-4}$  when  $\beta = 7.026$ . When  $\beta \approx 8.2$ , the eigenvalues turn around and start moving toward the origin. We see that they coalesce on the real axis at  $\beta \approx 10.2$ , and then split again, but confined to the real axis, with one eigenvalue converging to zero faster than the other. Notice that the eigenvalues remain unstable and real.

**4.4. Numerical results.** In this section, we (i) verify the results in [43], (ii) show that there are no additional unstable eigenvalues by Evans function computation with the energy estimates in section 3.2, and (iii) demonstrate that the unstable spectra stay unstable as they asymptotically approach the origin in the large exothermicity limit.

We first consider combustion fronts with  $\varepsilon = 0.1$  fixed and  $\beta$  varying between 7.026 and 14.1, while tracking the unstable roots of the Evans function. In each run, we performed a winding-number check using a closed semicircular contour to encapsulate the triangular region described in (22), thus guaranteeing that no other unstable eigenvalues exist. Then, by using the root-location method described in the above subsection, and when necessary taking successive small closed contours about the individual eigenvalues while regulating the relative error in the output, the moments are determined with high accuracy and the locations recorded.

For  $\varepsilon = 0.1$  and  $\beta = 7.026$ , two eigenvalues cross the imaginary axis at  $\lambda = \pm 6.8i \times 10^{-4}$ , thus verifying [43]. At  $\beta = 10.232$  the eigenvalues combine to form an eigenvalue of multiplicity 2 on the real axis, then split along the reals. After splitting one of them converges to the origin monotonically. The other eigenvalue first moves away from the origin but then turns back. They then travel toward the origin along the real line; see Figure 2. We remark that similar runs for other values of  $\varepsilon$  were performed, ranging from 0.05 to 1.0, and yielded the same qualitative outcome.

**Acknowledgments.** The authors thank the anonymous referees for their comments and suggestions. Ghazaryan thanks Peter Gordon for useful remarks.

#### REFERENCES

- [1] J. ALEXANDER, R. GARDNER, AND C. JONES, *A topological invariant arising in the stability analysis of travelling waves*, J. Reine Angew. Math., 410 (1990), pp. 167–212.
- [2] C. ALVAREZ-PEREIRA AND J. M. VEGA, *Global stability of a premixed reaction zone (time-dependent Liñán's problem)*, SIAM J. Math. Anal., 21 (1990), pp. 884–904.

- [3] C. ALVAREZ-PEREIRA AND J. M. VEGA, *On the pulsating instability of two-dimensional flames*, European J. Appl. Math., 3 (1992), pp. 55–73.
- [4] G. BADER AND U. ASCHER, *A new basis implementation for a mixed order boundary value ODE solver*, SIAM J. Sci. Statist. Comput., 8 (1987), pp. 483–500.
- [5] S. BALASURIYA, G. GOTTLWALD, J. HORNIBROOK, AND S. LAFORTUNE, *High Lewis number combustion wavefronts: A perturbative Melnikov analysis*, SIAM J. Appl. Math., 67 (2007), pp. 464–486.
- [6] B. BARKER, J. HUMPHERRYS, AND K. ZUMBRUN, *STABLAB: A MATLAB-Based Numerical Library for Evans Function Computation*, <http://www.impact.byu.edu/stablab/> (July 2009).z
- [7] H. BERESTYCKI, B. NICOLAENKO, AND B. SCHEURER, *Traveling wave solutions to combustion models and their singular limits*, SIAM J. Math. Anal., 16 (1985), pp. 1207–1242.
- [8] J. BILLINGHAM, *Phase plane analysis of one-dimensional reaction diffusion waves with degenerate reaction terms*, Dyn. Stab. Syst., 15 (2000), pp. 23–33.
- [9] A. R. BISHOP, M. G. FOREST, D. W. McLAUGHLIN, AND E. A. OVERMAN II, *A quasiperiodic route to chaos in a near-integrable PDE*, Phys. D, 23 (1986), pp. 293–328.
- [10] T. BODDINGTON, A. COTTRELL, AND P. LAYE, *A numerical model of combustion in gasless pyrotechnic systems*, Combust. Flame, 76 (1989), pp. 63–69.
- [11] J. C. BRONSKI, *Semiclassical eigenvalue distribution of the Zakharov-Shabat eigenvalue problem*, Phys. D, 97 (1996), pp. 376–397.
- [12] J. BUCKMASTER AND G. LUDFORD, *Theory of Laminar Flames*, Cambridge University Press, Cambridge, UK, 1982.
- [13] A. DAVEY, *An automatic orthonormalization method for solving stiff boundary value problems*, J. Comput. Phys., 51 (1983), pp. 343–356.
- [14] E. DOEDEL, A. CHAMPNEYS, T. FAIRGRIEVE, Y. KUZNETSOV, B. SANDSTEDE, AND X. WANG, *Auto97: Continuation and Bifurcation Software for Ordinary Differential Equations*, Technical report, Concordia University, 1997.
- [15] L. O. DRURY, *Numerical solution of Orr-Sommerfeld-type equations*, J. Comput. Phys., 37 (1980), pp. 133–139.
- [16] J. W. EVANS AND J. A. FEROE, *Traveling waves of infinitely many pulses in nerve equations*, Math. Biosci., 37 (1977), pp. 23–50.
- [17] N. FENICHEL, *Geometric singular perturbation theory for ordinary differential equations*, J. Differential Equations, 31 (1979), pp. 53–98.
- [18] P. FIFE, *Mathematical Aspects of Reacting and Diffusing Systems*, in Lecture Notes in Biomath. 28, Springer, New York, 1979.
- [19] A. GHAZARYAN AND C. JONES, *On the stability of high Lewis number combustion fronts*, Discrete Contin. Dynam. Systems, 24 (2009), pp. 809–826.
- [20] A. GHAZARYAN AND C. JONES, *On the existence of high Lewis number combustion fronts*, Math. Comput. Simulation, 82 (2012), pp. 1133–1141.
- [21] A. GHAZARYAN, Y. LATUSHKIN, S. SCHETTER, AND A. J. DE SOUZA, *Stability of gasless combustion fronts in one-dimensional solids*, Arch. Ration. Mech. Anal., 198 (2010), pp. 981–1030.
- [22] A. GHAZARYAN, *Nonlinear stability of high Lewis number combustion fronts*, Indiana Univ. Math. J., 58 (2009), pp. 181–212.
- [23] N. HALE AND D. R. MOORE, *A Sixth-Order Extension to the MATLAB Package bvp4c of J. Kierzenka and L. Shampine*, Technical report NA-08/04, Oxford University Computing Laboratory, University of Oxford, Oxford, 2008.
- [24] D. HENRY, *Geometric Theory of Semilinear Parabolic Equations*, in Lecture Notes in Math. 840, Springer-Verlag, Berlin, 1981.
- [25] J. HUMPHERRYS, B. SANDSTEDE, AND K. ZUMBRUN, *Efficient computation of analytic bases in Evans function analysis of large systems*, Numer. Math., 103 (2006), pp. 631–642.
- [26] J. HUMPHERRYS AND K. ZUMBRUN, *An efficient shooting algorithm for Evans function calculations in large systems*, Phys. D, 220 (2006), pp. 116–126.
- [27] W. JOHNSON, *On a first-order boundary value problem from laminar flame theory*, Arch. Ration. Mech. Anal., 13 (1963), pp. 46–54.
- [28] C. K. R. T. JONES, *Geometric singular perturbation theory*, in Dynamical Systems, Lecture Notes in Math. 1609, Springer, Berlin, 1995, pp. 44–118.
- [29] Y. I. KANEL, *On steady state solutions to systems of equations arising in combustion theory*, Dokl. Akad. Nauk SSSR, 149 (1963), pp. 367–369.
- [30] T. KATO, *Perturbation Theory for Linear Operators*, in Classics in Mathematics, Springer-Verlag, Berlin, 1995.
- [31] V. LEDOUX, S. J. A. MALHAM, J. NIESEN, AND V. THÜMMLER, *Computing stability of multidimensional traveling waves*, SIAM J. Appl. Dyn. Syst., 8 (2009), pp. 480–507.

- [32] V. LEDOUX, S. J. A. MALHAM, AND V. THÜMMLER, *Grassmannian spectral shooting*, Math. Comp., 79 (2010), pp. 1585–1619.
- [33] E. LOGAK AND V. LOUBEAU, *Travelling wave solutions to a condensed phase combustion model*, Asymptot. Anal., 12 (1996), pp. 259–294.
- [34] E. LOGAK, *Mathematical analysis of a condensed phase combustion model without ignition temperature*, Nonlinear Anal., 28 (1997), pp. 1–38.
- [35] S. B. MARGOLIS AND B. MATKOWSKY, *Nonlinear stability and bifurcations in the transition from laminar to turbulent flame propagation*, Combust. Sci. Tech., 34 (1983), pp. 45–77.
- [36] S. B. MARGOLIS, *The transition to nonsteady deflagration in gasless combustion*, Progr. Energy Combust. Sci., 17 (1991), pp. 135–162.
- [37] M. MARION, *Etude mathématique d'un modèle de flamme laminaire sans température d'ignition: I - cas scalaire*, Ann. Fac. Sci. Toulouse, 6 (1984), pp. 215–255.
- [38] M. MARION, *Qualitative properties of a nonlinear system for laminar flames without ignition temperature*, Nonlinear Anal., 9 (1985), pp. 1269–1292.
- [39] B. J. MATKOWSKY AND D. O. OLAGUNJU, *Propagation of a pulsating flame front in a gaseous combustible mixture*, SIAM J. Appl. Math., 39 (1980), pp. 290–300.
- [40] B. J. MATKOWSKY AND D. O. OLAGUNJU, *Traveling waves along the front of a pulsating flame*, SIAM J. Appl. Math., 42 (1982), pp. 486–501.
- [41] B. J. MATKOWSKY AND G. I. SIVASHINSKY, *Propagation of a pulsating reaction front in solid fuel combustion*, SIAM J. Appl. Math., 35 (1978), pp. 465–478.
- [42] D. W. MC LAUGHLIN AND E. A. OVERMAN, II, *Whiskered tori for integrable PDEs: Chaotic behavior in near integrable PDE's*, in Surveys in Appl. Math. 1, Plenum, New York, 1995, pp. 83–203.
- [43] G. N. MERCER, H. S. SIDHU, R. O. WEBER, AND V. GUBERNOV, *Evans function stability of combustion waves*, SIAM J. Appl. Math., 63 (2003), pp. 1259–1275.
- [44] E. A. OVERMAN, II, D. W. MC LAUGHLIN, AND A. R. BISHOP, *Coherence and chaos in the driven damped sine-Gordon equation: Measurement of the soliton spectrum*, Phys. D, 19 (1986), pp. 1–41.
- [45] A. PAZY, *Semigroups of Linear Operators and Applications to Partial Differential Equations*, in Applied Mathematical Sciences 44, Springer-Verlag, New York, 1983.
- [46] P. SIMON, J. MERKIN, AND S. SCOTT, *Bifurcations in non-adiabatic flame propagation models*, in Focus on Combustion Research, S. Z. Jiang, ed., Nova Science, New York, 2006, pp. 315–357.
- [47] K. UCHIYAMA, *The behavior of solutions of some nonlinear diffusion equations for large time*, J. Math. Kyoto Univ., 183 (1978), pp. 453–508.
- [48] F. VARAS AND J. M. VEGA, *Linear stability of a plane front in solid combustion at large heat of reaction*, SIAM J. Appl. Math., 62 (2002), pp. 1810–1822.
- [49] R. O. WEBER, G. N. MERCER, H. S. SIDHU, AND B. F. GRAY, *Combustion waves for gases ( $Le = 1$ ) and solids ( $Le \rightarrow \infty$ )*, Roy. Soc. Lond. Proc. Ser. A Math. Phys. Eng. Sci., 453 (1997), pp. 1105–1118.
- [50] F. A. WILLIAMS, *Combustion Theory*, Benjamin, New York, 1985.
- [51] K. ZUMBRUN, *A local greedy algorithm and higher-order extensions for global numerical continuation of analytically varying subspaces*, Quart. Appl. Math., 68 (2010), pp. 557–561.